

Synthesis, Spectral and DFT Characterization, PASS Predication, Antimicrobial, and ADMET Studies of Some Novel Mannopyranoside Esters

Mohammed Mahbubul Matin*, and Priyanka Chakraborty
Bioorganic and Medicinal Chemistry Laboratory, Department of Chemistry, Faculty of Science, University of Chittagong, Chattogram 4331, Bangladesh

Abstract

Due to the biodegradability and drug-likeness properties, sugar esters (SEs) are getting especial attention from synthetic and bioorganic chemists. In this context, several 6-O-pentanoyl mannopyranoside esters (5-9) with alkanoyl and sulfonyl chains were synthesized reasonably in good yields. Both the prediction of activity spectra for substances (PASS) and in vitro tests indicated that these mannopyranoside esters possess better potentiality against fungal pathogens than the bacterial organisms. These SEs were also optimized with quantum chemical density functional theory (DFT), and various thermodynamic properties like frontier molecular orbital, and molecular electrostatic potential (MEP) were calculated and discussed. Absorption, distribution, metabolism, excretion, and toxicity (ADMET) calculations indicated that these SEs can pass through blood brain barrier and are less toxic. Drug-likeness results indicated good conditions for alkanoyl esters rather than sulfonyl esters despite their promising antifungal results. All the in vitro and in silico results indicated that the combination of pentanoyl (C5) and lauroyl (C12) chains in mannopyranoside framework, as in 9, might be a potential candidate for novel antifungal agent.

Keywords: Methyl α -D-mannopyranoside, Selective acylation, Antimicrobial agents, DFT calculations, ADMET.

1. Introduction

Carbohydrates, the most abundant group of compounds found in nature, participate in numerous biological processes such as anticoagulant, antigen, and hormones due to their highly specific interaction with the physiological receptors [1-2]. Considering their diverse biological events, several classes of derivatives like monosaccharide-based sugar esters (SEs) [3], amino-sugars [4], halogenated sugars [5] were synthesized and applied. Of them, SEs are composed of a carbohydrate moiety and one or more fatty acid parts. The SEs have attracted particular interest as they are non-toxic, biodegradable, non-allergic, and non-irritating [6-7]. In the last few decades, promising antimicrobial properties of SEs have been reported to have several advantages over conventional multidrug resistant (MDR) antimicrobial agents [8-10]. Hence, SEs are becoming widely used in food additives, pharmaceutical, cosmetics, and personal care products [8, 11].

For example, Lee et al. [12] showed that lactose esters esterified with decanoic and lauric acids exhibited greater microbial inhibitory properties than lactose. Kabir and co-workers [13-15] also synthesized and evaluated antimicrobial potentiality of several mannofuranoside (1, Figure 1) and

* Corresponding author. Tel.: +880-1716-839689; fax: +880-31-2606014
E-mail address: mahbubchem@cu.ac.bd; mmmatin2004@yahoo.co.in

Manuscript History:

Received 06 October, 2020, Revised 17 October, 2020, Accepted 17 October, 2020, Published 30 October, 2020

mannopyranoside (**2**) esters. They found that in the furanose form, all these esters were weak inhibitors against tested pathogens whereas in the pyranose form of mannopyranoside, esters were more susceptible against microorganisms especially against fungal pathogens [13-16]. The higher reactivity of the pyranose SEs compared to the furanose SEs was further supported by AlFindee et al. [8]. Amongst the tested SEs, they [8] found that mannopyranose lauroate **3** (Figure 1) was highly active against methicillin-resistant *Staphylococcus aureus* ATCC 33591 (MRSA).

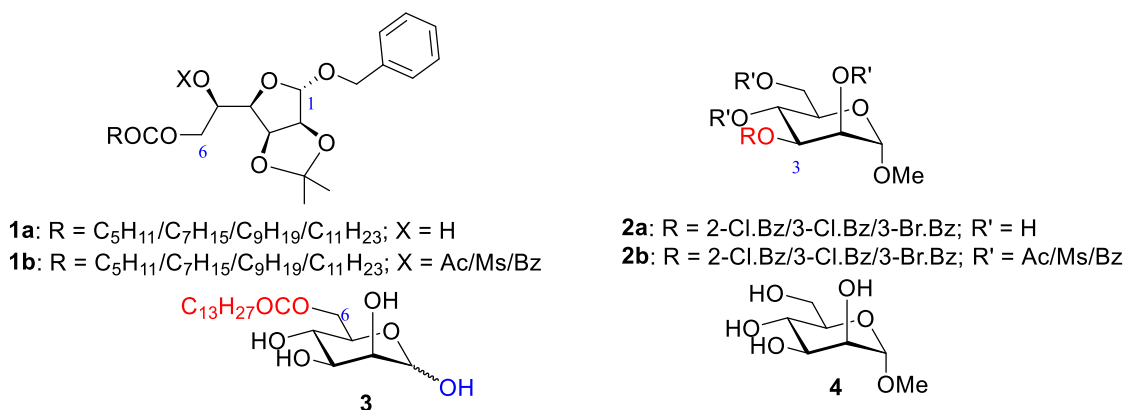


Figure 1. Structure of bioactive MDM esters.

Various methods for selective and regioselective esterification were reported [17-18]. However, the tremendous variation of carbohydrate structures and the presence of several 2° hydroxyl groups affect the selective esterification process [19]. Generally, direct esterification (acylation) is preferred over other methods as it can avoid complex processes of multiple steps, is inexpensive, and provides higher yields [20-21]. Again, there is a lack of consensus about the structure activity relationship (SAR) such as which acyl chain(s) of the SEs is the most susceptible to which organism [22]. In the search of novel and applied methods [23-24] in the field of bioorganic and drug design, five new SEs (**5-9**) with different groups starting from methyl α -D-mannopyranoside (**4**, Figure 1) were synthesized, and tested the *in vitro* antimicrobial potentiality along with pharmacokinetic, and ADMET properties.

2. Materials and methods

2.1. Instrumentation and methods

All the reagents such as methyl α -D-mannopyranoside (**4**), pentanoyl chloride, mesyl chloride, benzoyl chloride, tosyl chloride and lauroyl chloride were analytically graded and purchased from Merck (Germany). The solvents (methanol, *n*-hexane, ethyl acetate etc.) are commercially available (Merck) and used as purchased unless otherwise specified. Evaporations were conducted below 40 °C in a Buchi rotary evaporator (R-100, Switzerland) under diminished pressure. TLC (thin layer chromatography) was performed on Kieselgel GF₂₅₄ plates, and the plates were heated at 140–200 °C by spraying with methanolic H₂SO₄ (1%) until coloration took place. CC (column chromatography) was performed with silica gel G₆₀. The solvent system employed for the TLC and CC was chloroform/methanol and/or *n*-hexane/ethyl acetate in different proportions. FT-IR spectra were recorded on a FT-IR spectrophotometer (Shimadzu, IR Prestige-21) in KBr technique. ¹H (400 MHz) and ¹³C (100 MHz) NMR spectra were recorded in CDCl₃ solution using tunable multinuclear probe (Bruker DPX-400 spectrometer, Switzerland) at Jahangirnagar University, Dhaka. TMS (tetramethylsilane) as an internal standard for NMR and the chemical shifts were reported in δ scale (ppm). The coupling constants (*J*) values were shown in Hz and the elemental analyses were conducted with a C,H-analyzer.

2.2. Synthesis

2.2.1. Methyl 6-*O*-pentanoyl- α -D-mannopyranoside (5)

The title compound was prepared from the unimolar reaction of methyl α -D-mannopyranoside (MDM, **4**) and pentanoyl chloride (1.1 molar eq) in dry pyridine for 16 h in 79% yield as a semi-solid using the literature procedure [25].

2.2.2. General procedure for the 2,3,4-tri-*O*-acylation of pentanoate 5

Acyl halide (3.3 eq.) was slowly added to a stirred solution of pentanoate **5** (0.1 g) in dry pyridine (1 mL) at 0 °C followed by addition of catalytic amount of DMAP. The reaction mixture was allowed to attain room temperature and stirring was continued further for 8-14 h. In case of compound **9**, the reaction mixture was stirred for an additional 1 h at 45 °C. A few drops of cooled water were added to the reaction mixture to decompose excess acyl halide. The reaction mixture was extracted with dichloromethane (DCM, 4×3 mL) followed by washing with 5% hydrochloric acid, saturated aqueous sodium hydrogen carbonate solution and brine. The organic layer was dried and concentrated in a rotavapor. The residue, thus obtained, on CC (gradient elution from *n*-hexane to *n*-hexane/ethyl acetate = 10:1) gave the corresponding 2,3,4-tri-*O*-acyl esters (**6-9**).

Methyl 2,3,4-tri-*O*-mesyl-6-*O*-pentanoyl- α -D-mannopyranoside (**6**): Semi-solid (turned pale-yellow after a couple of days); yield 93%; $R_f = 0.47$ (*n*-hexane/EA = 4/1); FT-IR (KBr): 1747 (CO), 1367, 1362(2) (SO₂), 1081 cm⁻¹ (pyranose ring). ¹H NMR (400 MHz, CDCl₃): δ_H 5.36 (1H, dd, $J = 9.2$ and 3.4 Hz, H-3), 5.30 (1H, t, $J = 9.2$ Hz, H-4), 5.25 (1H, dd, $J = 3.4$ and 1.4 Hz, H-2), 4.71 (1H, d, $J = 1.4$ Hz, H-1), 4.33 (1H, dd, $J = 12.0$ and 5.6 Hz, H-6a), 4.13 (1H, dd, $J = 12.0$ and 2.4 Hz, H-6b), 3.99 (1H, ddd, $J = 9.2$, 5.6 and 2.4 Hz, H-5), 3.44 (3H, s, OCH₃), 3.38 (s, 3H, SO₂CH₃), 3.33 (s, 3H, SO₂CH₃), 3.23 (s, 3H, SO₂CH₃), 2.40 [2H, t, $J = 7.6$ Hz, CH₃(CH₂)₂CH₂CO], 1.58-1.65 (2H, m, CH₃CH₂CH₂CH₂CO), 1.34-1.41 [2H, m, CH₃CH₂(CH₂)₂CO], 0.93 [3H, t, $J = 7.4$ Hz, CH₃(CH₂)₃CO]. ¹³C NMR (100 MHz, CDCl₃): δ_C 173.6 [CH₃(CH₂)₃CO], 98.9 (C-1), 69.4, 68.8, 68.5, (C-2/C-3/C-5), 66.7 (C-4), 62.6 (C-6), 55.2 (OCH₃), 38.8, 38.6(2) (3×SO₂CH₃), 33.9 [CH₃(CH₂)₂CH₂CO], 27.1 (CH₃CH₂CH₂CH₂CO), 22.2 [CH₃CH₂(CH₂)₂CO], 13.9 [CH₃(CH₂)₃CO]. Anal. Calcd for C₁₅H₂₈O₁₃S₃ (512.56): C, 35.15; H, 5.51. Found: C, 35.19; H, 5.53.

Methyl 2,3,4-tri-*O*-benzoyl-6-*O*-pentanoyl- α -D-mannopyranoside (**7**): Clear syrup; yield 86%; $R_f = 0.53$ (*n*-hexane/EA = 4/1); FT-IR (KBr): 1755, 1740, 1735, 1733 (CO), 1068 cm⁻¹ (pyranose ring). ¹H NMR (400 MHz, CDCl₃): δ_H 8.12 (2H, d, $J = 7.2$ Hz, Ar-*H*), 7.97 (2H, d, $J = 8.4$ Hz, Ar-*H*), 7.85 (2H, d, $J = 8.4$ Hz, Ar-*H*), 7.48-7.54 (2H, m, Ar-*H*), 7.36-7.45 (5H, m, Ar-*H*), 7.24-7.30 (2H, m, Ar-*H*), 5.97 (1H, t, $J = 10.0$ Hz, H-4), 5.90 (1H, dd, $J = 10.0$ and 3.2 Hz, H-3), 5.70 (1H, dd, $J = 3.2$ and 1.2 Hz, H-2), 5.01 (1H, d, $J = 1.2$ Hz, H-1), 4.29-4.37 (3H, m, H-5, H-6a and H-6b), 3.55 (3H, s, OCH₃), 2.34-2.39 [2H, m, CH₃(CH₂)₂CH₂CO], 1.60-1.68 (2H, m, CH₃CH₂CH₂CH₂CO), 1.28-1.39 [2H, m, CH₃CH₂(CH₂)₂CO], 0.91 [3H, t, $J = 7.2$ Hz, CH₃(CH₂)₃CO]. Anal. Calcd for C₃₃H₃₄O₁₀ (590.63): C, 67.11; H, 5.80. Found: C, 67.17; H, 5.82.

Methyl 6-*O*-pentanoyl-2,3,4-tri-*O*-tosyl- α -D-mannopyranoside (**8**): Syrup; yield 88%; $R_f = 0.55$ (*n*-hexane/EA = 4/1); FT-IR (KBr): 1740 (CO), 1371, 1369, 1368 (SO₂), 1075 cm⁻¹ (pyranose ring). ¹H NMR (400 MHz, CDCl₃): δ_H 7.81 (2H, d, $J = 8.0$ Hz, Ar-*H*), 7.75 (2H, d, $J = 8.0$ Hz, Ar-*H*), 7.62 (2H, d, $J = 8.0$ Hz, Ar-*H*), 7.32-7.40 (4H, m, Ar-*H*), 7.29 (2H, d, $J = 7.8$ Hz, Ar-*H*), 4.94 (1H, t, $J = 9.6$ Hz, H-4), 4.88 (1H, d, $J = 1.6$ Hz, H-1), 4.84 (1H, dd, $J = 3.2$ and 1.6 Hz, H-2), 4.81 (1H, dd, $J = 9.6$ and 3.2 Hz, H-3), 4.34 (1H, dd, $J = 12.0$ and 2.0 Hz, H-6a), 4.02 (1H, dd, $J = 12.2$ and 4.8 Hz, H-6b), 3.80-3.85 (1H, m, H-5), 3.34 (3H, s, OCH₃), 2.48 (3H, s, CH₃C₆H₄SO₂), 2.46 (6H, s, 2×CH₃C₆H₄SO₂), 2.33 [2H, t, $J = 7.2$ Hz, CH₃(CH₂)₂CH₂CO], 1.57-1.67 (2H, m, CH₃CH₂CH₂CH₂CO), 1.31-1.40 [2H, m, CH₃CH₂(CH₂)₂CO], 0.92 [3H, t, $J = 7.6$ Hz, CH₃(CH₂)₃CO]. Anal. Calcd for C₃₃H₄₀O₁₃S₃ (740.85): C, 53.50; H, 5.44. Found: C, 53.54; H, 5.49.

Methyl 2,3,4-tri-*O*-lauroyl-6-*O*-pentanoyl- α -D-mannopyranoside (**9**): Semi-solid; yield 80%; R_f = 0.68 (*n*-hexane/EA = 4:1); FT-IR (KBr) $\nu_{\max}/\text{cm}^{-1}$: 1745, 1721, 1718, 1714 (C=O), 1068 (pyranose ring). ^1H NMR (400 MHz, CDCl_3): δ_{H} 5.38 (dd, J = 9.9 and 3.2 Hz, 1H, H-3), 5.33 (t, J = 9.8 Hz, 1H, H-4), 5.27 (dd, J = 3.2 and 1.2 Hz, 1H, H-2), 4.68 (d, J = 1.2 Hz, 1H, H-1), 4.21 (dd, J = 12.0 and 5.4 Hz, 1H, H-6a), 4.14 (dd, J = 12.0 and 2.2 Hz, 1H, H-6b), 3.93-3.97 (m, 1H, H-5), 3.42 (s, 3H, OCH_3), 2.28-2.43 [m, 8H, $\text{CH}_3(\text{CH}_2)_2\text{CH}_2\text{CO}$ and $3\times\text{CH}_3(\text{CH}_2)_9\text{CH}_2\text{CO}$], 1.55-1.66 [m, 8H, $\text{CH}_3\text{CH}_2\text{CH}_2\text{CH}_2\text{CO}$ and $3\times\text{CH}_3(\text{CH}_2)_8\text{CH}_2\text{CH}_2\text{CO}$], 1.20-1.43 [br m, 50H, $\text{CH}_3\text{CH}_2(\text{CH}_2)_2\text{CO}$ and $3\times\text{CH}_3(\text{CH}_2)_8(\text{CH}_2)_2\text{CO}$], 0.94 (t, J = 7.4 Hz, 3H, CH_3), 0.90 (t, J = 7.2 Hz, 9H, $3\times\text{CH}_3$). ^{13}C NMR (100 MHz, CDCl_3): δ_{C} 173.5, 172.7, 172.5, 172.4 [$\text{CH}_3(\text{CH}_2)_3\text{CO}$ and $3\times\text{CH}_3(\text{CH}_2)_{10}\text{CO}$], 99.1 (C-1), 69.1, 68.9, 68.6, (C-2/C-3/C-5), 65.7 (C-4), 62.3 (C-6), 55.2 (OCH_3), 34.0(4) [$\text{CH}_3(\text{CH}_2)_2\text{CH}_2\text{CO}$ and $3\times\text{CH}_3(\text{CH}_2)_9\text{CH}_2\text{CO}$], 32.0, 31.8(2) [$3\times\text{CH}_3(\text{CH}_2)_8\text{CH}_2\text{CH}_2\text{CO}$], 29.4(3), 29.2 (6), 29.1(3) 29.0(3) [$3\times\text{CH}_3(\text{CH}_2)_3(\text{CH}_2)_5(\text{CH}_2)_2\text{CO}$], 26.8 ($\text{CH}_3\text{CH}_2\text{CH}_2\text{CH}_2\text{CO}$), 25.1(3), 24.6(3) [$3\times\text{CH}_3\text{CH}_2(\text{CH}_2)_2(\text{CH}_2)_8\text{CO}$], 22.5(4) [$\text{CH}_3\text{CH}_2(\text{CH}_2)_2\text{CO}$ and $3\times\text{CH}_3\text{CH}_2(\text{CH}_2)_9\text{CO}$], 14.0(4) [$\text{CH}_3(\text{CH}_2)_3\text{CO}$ and $3\times\text{CH}_3(\text{CH}_2)_{10}\text{CO}$]. Anal. Calcd for $\text{C}_{48}\text{H}_{88}\text{O}_{10}$ (825.22): C, 69.86; H, 10.75. Found: C, 69.80; H, 10.81.

2.3. PASS predication

Web based PASS (prediction of activity spectra for substances; <http://www.pharmaexpert.ru/PASSonline/index.php>) was used for the prediction of a plethora of biological activities [26]. This program was designed to anticipate a plethora of biological activities with 90% accuracy. The structures of the SEs were drawn with ChemDraw 16.0, and then converted into their SD file format and used to predict biological spectrum using PASS online version [27]. The result was presented as Pa (probability for active compound) and Pi (probability for inactive compound). Here, $\text{Pa} > \text{Pi}$ is considered in the scale 0.000 to 1.000 and in general, $\text{Pa} + \text{Pi} \neq 1$.

2.4. *In vitro* antimicrobial activity test

For the antibacterial activity test one Gram-positive bacteria (*Staphylococcus aureus* ATCC 25923) and two Gram-negative bacteria (*Escherichia coli* ATCC 25922, *Pseudomonas aeruginosa* CRL, ICDDR,B) were used. Antibacterial activity was measured as diameter of zone of inhibition using the disc diffusion method [28-30]. Mueller-Hinton (agar and broth) medium was used to culture the bacteria. The petri-plates (70 mm in diameter) were incubated at 37 °C for 48 h. The sterilized paper discs were soaked with a 2% solution of each compound in dimethylformamide (DMF) at the rate of 100 μg (dry weight) per disc. At this stage, the petri-plates with paper disc were kept for 4 h at low temperature (4 °C) and the test chemicals diffused from disc to the surrounding medium by this time. The plates were then incubated at (35 \pm 2) °C for the growth of test organisms and were observed at 24 h intervals for two days. The activity was measured in mm of diameter of zone of inhibition, and each experiment was carried out three times. Tetracycline (antibiotic used for bacterial infections, brand name Tetrax-500, from Square Pharmaceuticals Ltd., Bangladesh) was used as a positive control and compared with tested chemicals under identical conditions.

The *in vitro* antifungal efficacy was assessed employing the food poisoning technique [31-33] against two human pathogenic fungi (*Aspergillus fumigatus* ATCC 46645 and *Aspergillus niger* ATCC 16404). Potato dextrose agar (PDA) medium was used for the culture of these fungi. Necessary amount of medium was taken in a conical flask separately and was sterilized in autoclave (at 121 °C and 15 psi) for 15 minutes. The weighed amount of test chemical (2% in DMF) was added to the sterilized medium in conical flask with the necessary concentration followed by transferring 100 μL in sterilized glass petri dishes individually. Linear mycelial growth of fungus was measured after 2~4 days of incubation, and measured as percentage of zone of inhibition. Proper control was maintained separately and with sterilized PDA medium without chemical and three replications were prepared for

each treatment. The results were compared with the standard antifungal antibiotic, fluconazole (brand name Omastin, 50 mg, Beximco Pharmaceuticals Ltd., Bangladesh).

2.5. DFT calculations

In recent years, DFT (density function theory) based quantum mechanical methods are widely used to predict thermal energies, molecular orbital (MO), and molecular electrostatic potential (MEP) properties [21]. First of all, the basic geometry of methyl α -D-mannopyranoside (**4**) was taken from the online structure database named ChemSpider. Then the SEs **5-9** were drawn with the GaussView (5.0) program [34]. Using Gaussian 09 program, all the compounds were optimized at B3LYP/6-31G basis set of DFT. We have used GaussSum 3.0 to get DOS plot. To visualize MEP online WebMO demo server was used for all the compounds. FMO (frontier molecular orbital) energy like HOMO (highest occupied molecular orbital), LUMO (lowest unoccupied molecular orbital), HOMO-LUMO gap, hardness (η), and softness (S) were calculated at the same level of theory using the following equations:

$$\text{Gap} = [\varepsilon_{\text{LUMO}} - \varepsilon_{\text{HOMO}}]; \quad \eta = \frac{\varepsilon_{\text{LUMO}} - \varepsilon_{\text{HOMO}}}{2}; \quad S = \frac{1}{\eta}$$

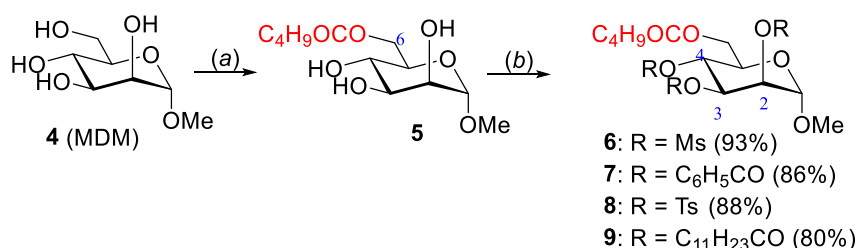
2.6. ADME/T analysis

In silico ADMET (absorption, distribution, metabolism, excretion, and toxicity) analyses were conducted by using computational approaches such as pkCSM program [9, 35]. This could avoid the tremendous cost and time associated with the *in vivo* experiments for drug discovery. Initially drawn SEs in ChemDraw 16.0 were converted to InChI Key, isomeric SMILES (simplified molecular-input line-entry system), and SD file formats. These formats were used to predict ADMET from online pkCSM-pharmacokinetics (<http://biosig.unimelb.edu.au>) [35] and SwissADME free web tools (<http://www.swissadme.ch>) [36].

3. Results and discussion

3.1. Synthesis of MDM esters 5-9

In addition to biological applications, mannopyranoside esters were also used as intermediate for the synthesis of other natural products [37-38]. Thus, methyl α -D-mannopyranoside (MDM, **4**) was directly treated with unimolar pentanoyl chloride in pyridine at low temperature for 16 h followed by chromatographic purification gave a semi-solid (Scheme 1). The compound was identified as methyl 6-*O*-pentanoyl- α -D-mannopyranoside (**5**) [25]. Having pentanoate **5** in hand, we have conducted its 2,3,4-tri-*O*-esterification with four different acylating agents using the direct method. Initial reaction of **5** with mesyl (methanesulfonyl) chloride for 8 h gave a semi-solid in 93% (Scheme 1).



Scheme 1. Reagents and conditions: (a) Py, C₄H₉COCl, 0 °C-rt, 18 h, 79% [25]; (b) MsCl/C₆H₅COCl/TsCl/C₁₁H₂₃COCl, Py, DMAP, 0 °C-rt, 8-14 h.

The FT-IR spectrum of the compound showed absence of hydroxyl stretching and exhibited characteristic bands at 1747 (CO), 1367 and 1362(2) (SO₂) cm⁻¹ indicating the complete mesylation of the molecule. In its ¹H NMR spectrum, the additional nine protons at δ 3.38 (s, 3H), 3.33 (s, 3H) and 3.23 (s, 3H) were due to the addition of three mesyl groups in the compound. This was further confirmed by analyzing its ¹³C NMR spectrum, where three mesyl carbons appeared at δ 38.8 and 38.6(2). Also, H-2, H-3 and H-4 protons shifted considerable down-fields at δ 5.25, 5.36 and 5.30, respectively as compared to its precursor compound **5** (H-2 at δ 3.92; H-3 at δ 3.78; H-4 at δ 3.64) [25]. This clearly indicated the attachment of three mesyl groups at C-2, C-3 and C-4 positions. These data in corroboration with elemental analyses established the structure of the semi-solid as methyl 2,3,4-tri-*O*-mesyl-6-*O*-pentanoyl-α-D-mannopyranoside (**6**).

In the next step, treatment of pentanote **5** with trimolar benzoyl chloride for 14 h followed by chromatography furnished a thick syrup in 86% yield (Scheme 1). Its FT-IR spectrum showed four carbonyl bands at 1755, 1740, 1735 and 1733 cm⁻¹, and absence of hydroxyl bands. In the ¹H NMR spectrum, fifteen aromatic protons appeared at δ 8.12 (2H), 7.97 (2H), 7.85 (2H), 7.48-7.54 (2H), 7.36-7.45 (5H) and 7.24-7.30 (2H). Also, H-2, H-3 and H-4 protons shifted down-fields than that of its precursor pentanoate **5** [25] indicating the attachment of benzoyl groups at C-2, C-3 and C-4 positions. Thus, the structure of the compound was assigned as methyl 2,3,4-tri-*O*-benzoyl-6-*O*-pentanoyl-α-D-mannopyranoside (**7**).

Similarly, the reaction of pentanoate **5** with tosyl (*p*-toluenesulfonyl) chloride in dry pyridine for 12 h gave a semi-solid in 88% (Scheme 1). In addition to one carbonyl signal at 1740 cm⁻¹, it showed sulphonyl stretching at 1371, 1369 and 1368 cm⁻¹ in its FT-IR spectrum which indicated the attachment of three tosyl groups in the molecule. This fact was confirmed by the appearance of the corresponding twelve aromatic protons and nine methyl protons in its ¹H NMR spectrum (Figure 2a). The complete spectral data in correlation with compound **6** and **7** led us to assign the structure of the compound as methyl 6-*O*-pentanoyl-2,3,4-tri-*O*-tosyl-α-D-mannopyranoside (**8**).

Finally, lauroylation of **5** with lauroyl chloride at 0-45 °C for 15 h yielded a semi-solid in 80% (Scheme 1). In its FT-IR spectrum, bands at 1745, 1721, 1718 and 1714 were due to the presence of four carbonyl groups. In the ¹H NMR spectrum, a three-proton singlet at δ 3.42 was due to the anomeric methoxy group. Appearance of additional sixty-nine protons in the aliphatic region indicated the attachment of three lauroyl groups in the molecule. In its ¹³C NMR spectrum, as shown in Figure 2b, a total of four carbonyl carbons resonated at δ 173.5, 172.7, 172.5 and 172.4 ppm, and thus, confirming the attachment of three new acyl groups in the compound. Complete analyses of all the spectra confirmed the structure of the molecule as methyl 2,3,4-tri-*O*-lauroyl-6-*O*-pentanoyl-α-D-mannopyranoside (**9**).

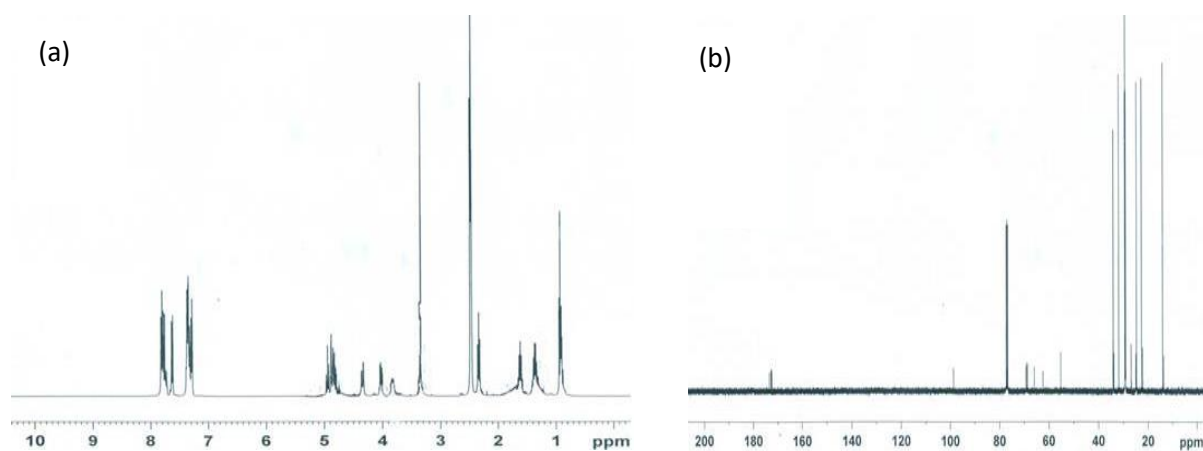


Figure 2. (a) ¹H NMR spectrum of compound **8**; (b) ¹³C NMR spectrum of compound **9**.

3.2. PASS predicted antimicrobial activities

After the successful synthesis of SEs **5-9**, we applied prediction of activity spectra for substances (PASS) for their activity test. PASS results in its designated as Pa and Pi form is presented in Table 1.

Table 1. Predicted biological activity of the SEs **5-9** using PASS software.

Drug	Biological activity							
	Antibacterial		Antifungal		Anti-carcinogenic		Antioxidant	
	Pa	Pi	Pa	Pi	Pa	Pi	Pa	Pi
4	0.541	0.013	0.628	0.016	0.731	0.008	0.667	0.004
5	0.528	0.014	0.669	0.012	0.769	0.006	0.530	0.005
6	0.408	0.028	0.436	0.042	0.433	0.026	0.228	0.025
7	0.505	0.016	0.642	0.014	0.632	0.011	0.413	0.011
8	0.362	0.040	0.388	0.052	0.299	0.098	0.263	0.032
9	0.551	0.012	0.673	0.011	0.614	0.012	0.463	0.008
TC	0.694	0.005	0.523	0.023	-	-	-	-
FZ	-	-	0.726	0.008	-	-	-	-

Pa = Probability 'to be active'; Pi = Probability 'to be inactive'; TC = tetracycline; FZ = fluconazole.

PASS predication (Table 1) of the mannopyranoside esters **5-9** were found $0.36 < Pa < 0.56$ for antibacterial and $0.38 < Pa < 0.68$ for antifungal. This indicated that these SEs should be more potent against fungi than that of bacterial pathogens. Also, the predicted antifungal potentiality of **5, 7** and **9** were better than the tetracycline while sulphonyl esters **6** and **8** were very poor. We have also checked anti-carcinogenic and antioxidant potentiality of these SEs. The PASS predication indicated $0.29 < Pa < 0.77$ for anti-carcinogenic and $0.26 < Pa < 0.53$ for antioxidant, which refers that the mannopyranoside esters might have better potentiality as anti-carcinogenic agents than that of antioxidant properties. Interestingly, PASS results showed better results for aliphatic and benzoyl esters (**5, 7, 9**) than sulphonyl esters (**6, 8**) in all the cases.

3.3. In vitro antimicrobial activities

3.3.1. Antibacterial activities

The *in vitro* antibacterial activities of the newly synthesized esters are presented in Table 2 (Figure 3).

Table 2. Antibacterial effects of **4-9**.

Diameter of zone of inhibition in mm (100 µg.dw / disc)			
Drug	<i>S. aureus</i>	<i>E. coli</i>	<i>P. aeruginosa</i>
4	08±0.50	NI	NI
5	08±0.50	NI	NI
6	07±1.00	NI	NI
7	07±0.55	NI	NI
8	08±0.35	NI	NI
9	06±0.50	NI	NI
TC ^[a]	*22±0.58	*25±0.50	*22±0.41

Zones are presented as (Mean±SD) (SD = standard deviation); TC = tetracycline; NI = no inhibition; dw = dry weight; * = good inhibition; [a] = standard antibiotic (25 µg/disc).

For the antibacterial test one Gram-positive (*Staphylococcus aureus*), and two Gram-negative (*Escherichia coli* and *Pseudomonas aeruginosa*) were used. It is evident that these SEs had very little antibacterial effects against *S. aureus* while none of the compounds showed any observable antibacterial effects against Gram-negative pathogens. The antibacterial results were found to be in consistent with PASS predicted results.

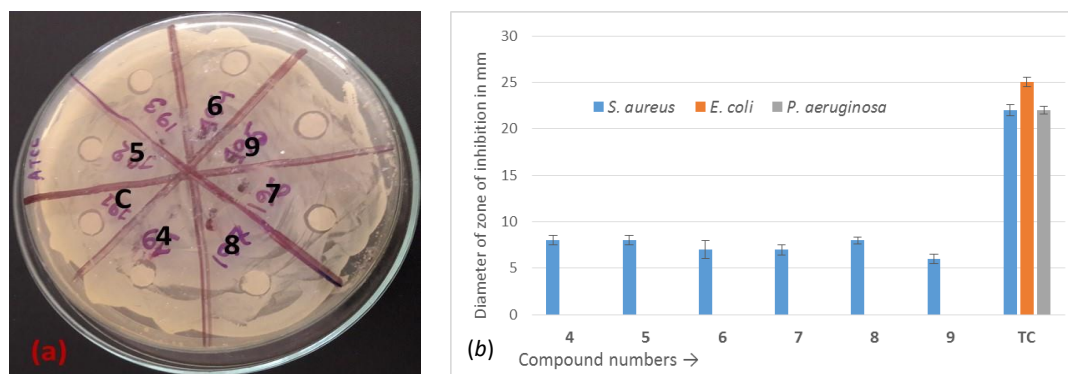


Figure 3. (a) Inhibition against *S. aureus* by the SEs 4-9; (b) Diameter of zone of inhibition in mm against bacteria by 4-9.

3.3.2. Antifungal activities

The *in vitro* antifungal activities of the SEs 5-9 were determined against two pathogenic fungi viz. *Aspergillus fumigatus* ATCC 46645, and *Aspergillus niger* ATCC 16404. The results, as shown in Table 3 (Figure 4), indicated that all the MDM esters had excellent antifungal activities as well as MDM 4. To be more precise, the SEs exhibited higher antifungal activities against *A. fumigatus* which were very similar and/or even better than that observed with standard antifungal drug fluconazole (Table 3). Lauroyl ester 9 showed the highest inhibition against both the organisms (*74.0% and *63.7%). Again, alkanoyl esters (5, 9) were found to be more prone than the sulphonyl esters (6, 8). More precisely, mannopyranoside esters were found to be more active against fungal pathogens than the bacterial organisms which were in complete agreement with the PASS predicted results (Table 1). It was observed that SEs with hydrophobic acyl chains showed better affinity with fungal enzyme (sterol 14 α -demethylase) than the bacterial enzymes which may lead to stop essential ergosterol biosynthesis, facilitating leaking of fungal cell membrane [21, 25].

Table 3. % of growth inhibition against fungal pathogens by 4-9.

Drug	wt. μ g/mL PDA	Percentage of zone of inhibition	
		<i>A. fumigatus</i>	<i>A. niger</i>
4	100	61.6 \pm 0.34	39.4 \pm 0.40
5	100	*71.7 \pm 0.68	39.2 \pm 0.64
6	100	*61.0 \pm 0.33	24.2 \pm 0.40
7	100	*63.3 \pm 0.54	27.3 \pm 0.33
8	100	*68.3 \pm 0.59	27.3 \pm 0.37
9	100	*74.0 \pm 0.82	*63.7 \pm 0.82
FZ ^[a]	12.5	*65.0 \pm 0.25	37.1 \pm 0.17

Inhibitions are presented as (Mean \pm SD). FZ = fluconazole; NI = no inhibition; dw = dry weight; * = good inhibition; [a] = standard antibiotic.

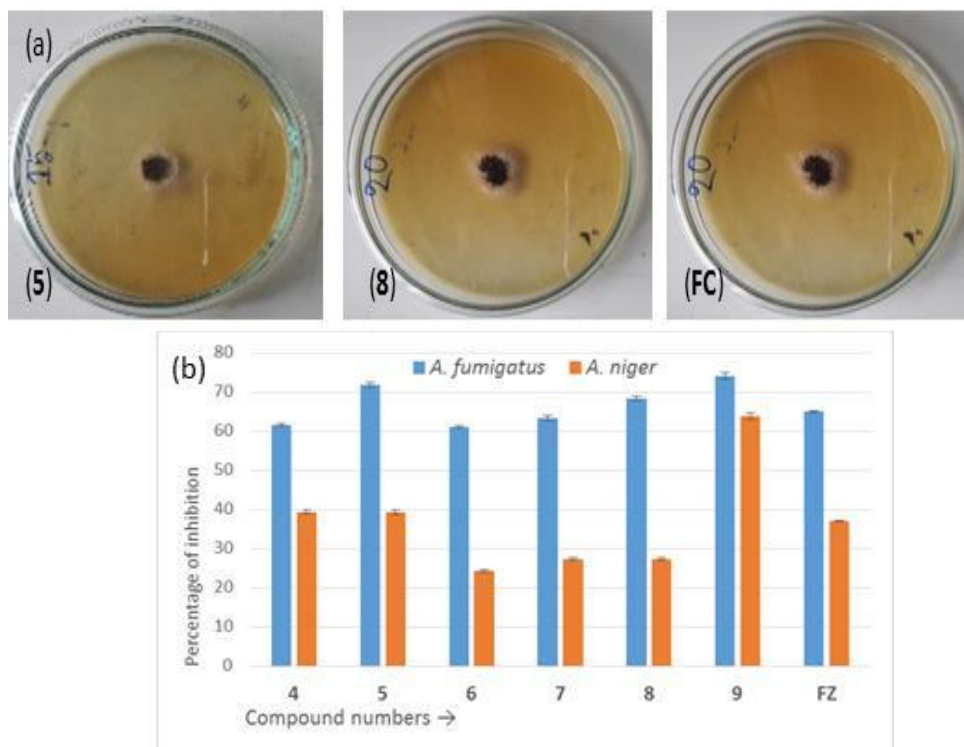


Figure 4. (a) Inhibition against *A. fumigatus* by the SEs 5, 8 and fluconazole; (b) Percentage of inhibition in mm against fungal pathogens.

3.4. DFT calculations: Thermodynamic properties

After successful synthesis and antimicrobial evaluation of SEs, we aimed to calculate their thermochemical properties optimizing with the Gaussian 09 program [34]. The density function theory (DFT, B3LYP/6-31G basis set) based optimized structure (298.15 K, 1.0 atm) of MDM 4 and its ester derivatives 5-9 are shown in Figure 5. All the compounds were found to possess 4C_1 conformation with similar C1 symmetry.

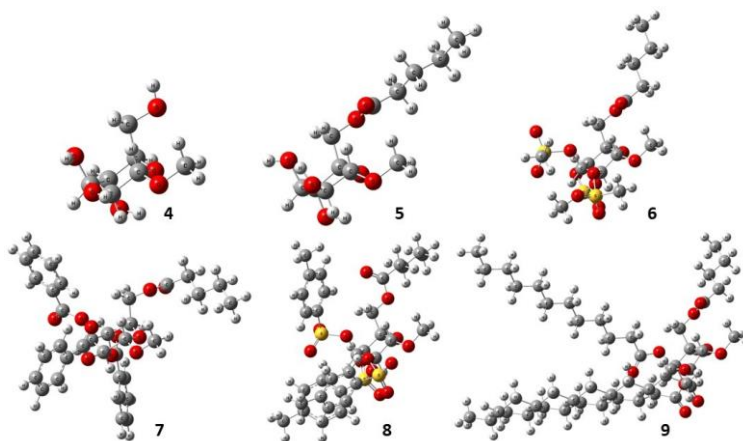


Figure 5. DFT optimized (B3LYP/6-311G) structures of 4-9.

Thermodynamic properties of these compounds such as electronic energy, enthalpy (ΔH), Gibbs free energy (G) and dipole moment (μ) calculated at 298.15 K are presented in Table 4. The greater

the value of negative energy, the more tightly the electron was bound to the nucleus. Here, the ester compounds **5-9** had greater negative electronic energy (-996.7523 to -3453.8907 Hartree) compared to the MDM **4** (-726.2243 Hartree) indicating that the addition of ester group increased the stability of the compounds. Tri-*O*-tosylate **9** with the highest negative electronic energy (-3453.8907 Hartree) indicated that it had the most tightly electron bound nucleus. Also, the SEs had lower ΔH values as compared to non-ester MDM **4** (Table 4) which further supported their increased stability. More precisely, these values were in consistent with the exothermic esterification reaction of carbohydrate molecules.

Again, Gibbs free energy (G) signifies spontaneity of a reaction when $G < 0$, and it combines enthalpy and entropy into a single value. It is evident from Table 4 that with the attachment and increase of acyl group(s) and bulkiness, the G (negative) values were increased which indicated their spontaneous binding, and interaction with other substrates. Finally, we calculated dipole moment (μ) of **4-9** which signified the measure of net molecular polarity and binding affinity. The increased μ as in the SEs **5-9** (4.3-9.0 Debye, Table 4) as compared to non-ester **4** (3.33 Debye) clearly demonstrated the higher binding affinity with target enzyme during antimicrobial activities and more polar nature of these molecules [6-7]. Amongst the synthesized esters, tosylate **9** was found to possess the highest thermodynamic properties (Table 4).

Table 4. Molecular formula (MF), molecular weight (MW, g/mol), electronic energy (EE), enthalpy, Gibbs free energy (GFE) and dipole moment (DM) of **4-9**.

Compound No.	MF	MW	EE (Hartree)	Enthalpy (Hartree)	GFE (Hartree)	DM (Debye)
4	C ₇ H ₁₄ O ₆	194.18	-726.2243	-725.9849	-726.0398	3.3323
5	C ₁₂ H ₂₂ O ₇	278.14	-996.7523	-996.3810	-996.4545	4.3482
6	C ₁₅ H ₂₈ O ₁₃ S ₃	512.56	-2760.7433	-2760.2412	-2760.3501	5.1533
7	C ₃₃ H ₃₄ O ₁₀	590.63	-2030.3235	-2029.6591	-2029.7835	4.0503
8	C ₃₃ H ₄₀ O ₁₃ S ₃	740.85	-3453.8907	-3453.1327	-3453.2852	9.0028
9	C ₄₈ H ₈₈ O ₁₀	825.22	-2633.6996	-2632.3005	-2632.5009	8.6106

3.4.1. Molecular orbitals (MO) analysis

Frontier molecular orbitals (FMO) such as HOMO (highest occupied molecular orbital) and LUMO (lowest unoccupied molecular orbital) are the orbitals that are most likely to be involved in chemical reactivity. The HOMO and LUMO energy levels of the SEs, as derived from DFT (B3LYP/6-31G) [39], is presented in Table 5 (Figure 6). It was clearly evident that the incorporation of benzoyl (**7**) and tosyl (**8**) ester moieties decreased the HOMO-LUMO gap compared to the parent mannopyranoside **4**. So, their hardness decreased and inversely softness increased. On the other hand, addition of pentanoyl (**5**), mesyl (**6**) and lauroyl (**9**) groups increased the HOMO-LUMO gap, and consequently increased their hardness and decreased softness.

Table 5. Energy (eV) of HOMO, LUMO, energy gap, hardness, and softness of SEs **4-9**.

Drug	ϵ HOMO	ϵ LUMO	Gap	Hardness (η)	Softness (S)
4	-7.014	-1.288	5.726	2.863	0.349
5	-6.926	-0.270	6.656	3.328	0.301
6	-7.476	-0.441	7.035	3.516	0.284
7	-6.967	-1.377	5.590	2.795	0.358
8	-7.004	-1.311	5.693	2.847	0.351
9	-7.157	-0.637	6.520	3.260	0.307

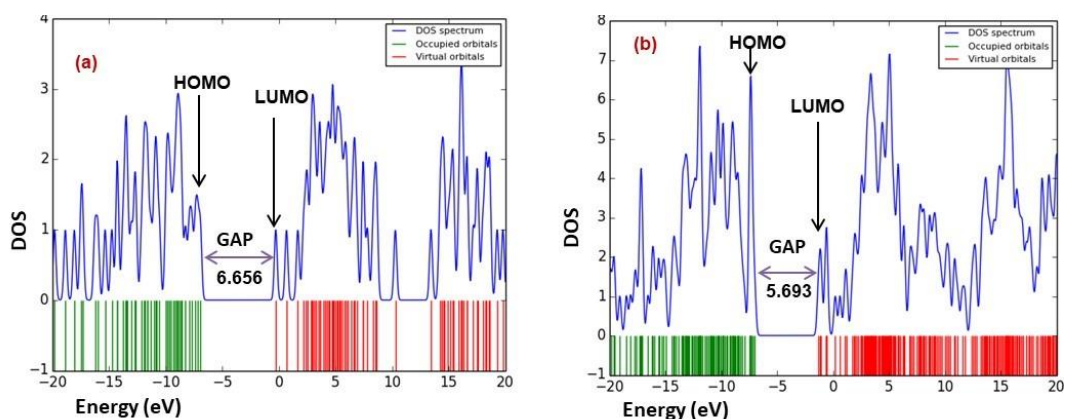


Figure 6. HOMO-LUMO energy gap and DOS plot of (a) **5**, and (b) **8**.

3.4.2. Molecular electrostatic potential (MEP) analysis

Molecular electrostatic potential (MEP) surface provides a visual representation of the possible reactive site of any compound. It is calculated to forecast the reactive sites for electrophilic and nucleophilic attack of all the optimized structures as shown in Figure 7. In general, red color represents maximum negative area which is a favorable site for electrophilic attack, blue color indicates the maximum positive area which is a favorable site for nucleophilic attack, and green color represents zero potential area. The negative potential region indicates excess electronegative atom (oxygen atoms), and positive potential region represents over hydrogen atoms. The MEP results (Figure 7) indicated that the incorporation of ester group(s) gradually increased the negative red color and thus imposed the maximum possibility for the electrophilic attack. In addition, the positive blue color increased for the sulfonyl (**6**, **8**) and lauroyl (**9**) esters indicating that only these SEs possess maximum nucleophilic attack site as compared to pentanoyl (**5**) and benzoyl (**7**) esters.

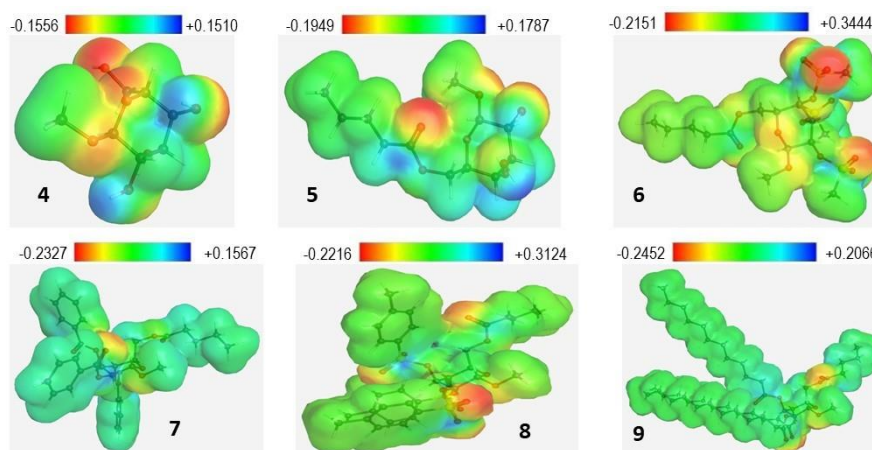


Figure 7. Molecular electrostatic potential (eV) of mannopyranosides **4-9**.

3.5. ADMET properties

Generally, absorption, distribution, metabolism, excretion, and toxicity (ADMET) constitute the pharmacokinetic profile of a drug molecule. It also plays a key role in the discovery/development of drugs, pesticides and related fields. Online based pkCSM program is used for the small-molecule pharmacokinetics prediction [35]. The ADMET properties, as presented in Table 6, indicated that SEs

6-9 had excellent human intestinal absorption (HIA) value. Distribution through BBB and CNS permeability indicated that these esters were comparable to that of fluconazole.

Table 6. ADMET calculation of mannopyranoside derived SEs **4-9**.

Drug	Absorption		P-gpI	Distribution		Metabolism CYP3A4 substrate	Excretion Total clearance	Toxicity	
	C2P	HIA (%)		BBB (permeability)	CNS			hERG inhibitor	Toxicity (LD ₅₀)
4	-0.247	33.43	No	-0.992	-3.622	No	0.671	No	1.157
5	-0.141	61.53	No	-1.076	-3.237	No	1.557	No	1.620
6	0.107	100	Yes	-2.807	-3.517	No	1.701	No	2.373
7	0.862	100	Yes	-1.608	-3.419	Yes	0.919	No	2.758
8	-0.151	100	Yes	-2.864	-3.981	Yes	0.626	No	2.557
9	0.631	100	Yes	-2.237	-2.598	Yes	1.968	No	2.541
FZ	1.191	87.82	No	-1.200	-3.221	No	0.386	No	2.21

C2P = Caco-2 permeability (log Papp in 10⁻⁶ cm/s, >0.90 indicates high permeability); HIA = Human intestinal absorption (% absorbed, >30% is better absorbed); P-gpI = P-glycoprotein inhibitor; BBB (blood brain barrier) is expressed in logBB (logBB >-1.0 is moderately cross blood brain barrier); CNS is expressed as logPS (logPS >-2.0 can easily penetrate the CNS); Total clearance is expressed in log mL/min/kg; Toxicity is calculated in oral rat acute toxicity (mol/kg); FZ = fluconazole.

Drug-likeness calculation was conducted using the SwissADME programme [36], and summarized in Table 7. We observed that the alkanoyl (**5, 9**) and benzoyl (**7**) SEs had good hydrogen bond donor and acceptor which was consistent with the Lipinski's rule of five [40]. However, sulphonyl esters **6** and **8** violated this rule. Topological polar surface area (TPSA) of a good drug should be less than 140 Å² [36]. The alkanoyl (**5, 9**) and benzoyl (**7**) esters had good TPSA value. However, sulfonyl esters **6** and **8** had higher TPSA (200.01 Å²) value. Although sulfonyl esters showed better antifungal activities, their drug likeness properties might not be suitable for good antimicrobial agents. Pan-assay interference compounds (PAINS) are chemical compounds that often give false positive results in high-throughput screens. However, all the SEs did not violate PAINS. Thus, ADME along with SwissADME indicated the better drug likeness conditions for alkanoyl esters especially 2,3,4-tri-*O*-lauroylmannopyranoside **9**.

Table 7. Calculation of drug-likeness using SwissADME.

Drug	HB acceptors	HB donors	TPSA Å ²	CYP1A2 inhibitor	CYP2C19 inhibitor	CYP2C9 inhibitor	CYP2D6 inhibitor	CYP3A4 inhibitor	PAINS alerts
4	6	4	99.38	No	No	No	No	No	0
5	7	3	105.45	No	No	No	No	No	0
6	13	0	200.01	No	No	No	Yes	No	0
7	10	0	123.66	No	Yes	Yes	Yes	Yes	0
8	13	0	200.01	No	No	No	No	Yes	0
9	10	0	123.66	No	No	No	No	No	0

*HB = Hydrogen bond, TPSA = Topological polar surface area, PAINS = Pan-assay interference compounds

4. Conclusion

Five new 6-*O*-pentanoyl- α -D-mannopyranoside esters (**5-9**) were synthesized and characterized through the use of spectroscopic techniques. PASS predication indicated that these esters had better antifungal potentiality and was confirmed by their *in vitro* antimicrobial tests. Structurally methyl 6-

O-pentanoyl-2,3,4-tri-*O*-lauroyl- α -D-mannopyranoside (**9**) was found to be the most potential antimicrobial agent. In this context, DFT based thermodynamic properties were calculated which indicated that addition of ester groups in mannopyranoside skeleton increased their dipole moment which was responsible for their higher binding affinity with the target enzyme during antimicrobial activities and more polar nature. ADMET and drug-likeness properties indicated that these SEs **6-9** had excellent human intestinal absorption (HIA) with lower toxicity. However, alkanoyl (**5**, **9**) and benzoyl (**7**) esters had better TPSA value than the sulfonyl esters (**6**, **8**). Thus, the present study might be helpful for designing mannopyranoside-based antifungal drug molecules.

Acknowledgements

We highly acknowledge the financial support from the Ministry of Education, Bangladesh and BANBEIS (grant no. PS 201660, 2016-17).

References

- [1] Boons, G. -J, & Hale, K. J. (2000). *Organic Synthesis with Carbohydrates*, Sheffield Academic Press Ltd.
- [2] Dhavale, D. D., Matin, M. M., Sharma, T. & Sabharwal, S. G. (2004). Synthesis and evaluation of glycosidase inhibitory activity of octahydro-2H-pyrido[1,2-a]pyrimidine and octahydro-imidazo[1,2-a]pyridine bicyclic diazasugars, *Bioorganic & Medicinal Chemistry*, Vol.12, No.15, 4039-4044.
- [3] Pöhnlein, M., Slomka, C., Kukhareenko, O., Gärtner, T., Wiemann, L. O., Sieber, V., Syldatk, C., & Hausmann, R. (2014). Enzymatic synthesis of amino sugar fatty acid esters, *European Journal of Lipid Science and Technology*, Vol.116, No.4, 423-428.
- [4] Miljkovic, M. (2010). Amino Sugars. In: *Carbohydrates: Synthesis, Mechanisms, and Stereoelectronic Effects*, Springer, New York, NY.
- [5] Uhrig, M. L., Lantaño, B., & Postigo, A. (2019). Synthetic strategies for fluorination of carbohydrates, *Organic & Biomolecular Chemistry*, Vol.17, No.21, 5173-5189.
- [6] Matin, M. M., Bhuiyan, M. M. H., Kabir, E., Sanaullah, A. F. M., Rahman, M. A., Hossain, M. E., & Uzzaman, M. (2019). Synthesis, characterization, ADMET, PASS predication, and antimicrobial study of 6-*O*-lauroyl mannopyranosides, *Journal of Molecular Structure*, Vol.1195, 189-197.
- [7] Matin, M. M., Bhattacharjee, S. C., Chakraborty, P., & Alam, M. S. (2019). Synthesis, PASS predication, *in vitro* antimicrobial evaluation and pharmacokinetic study of novel *n*-octyl glucopyranoside esters, *Carbohydrate Research*, Vol.485, 107812.
- [8] AlFindee, M. N., Zhang, Q., Subedi, Y. P., Shrestha, J. P., Kawasaki, Y., Grilley, M., Taemoto, J. Y., & Chang, C. W. T. (2018). One-step synthesis of carbohydrate esters as antibacterial and antifungal agents, *Bioorganic & Medicinal Chemistry*, Vol.26, 765-774.
- [9] Matin, M. M., Roshid, M. H. O., Bhattacharjee, S. C., & Azad, A. K. M. S. (2020). PASS predication, antiviral, *in vitro* antimicrobial, and ADMET studies of rhamnopyranoside esters, *Medical Research Archives*, Vol.8, No.7, 2165.
- [10] Matin, M. M. (2014). Synthesis and antimicrobial study of some methyl 4-*O*-palmitoyl- α -L-rhamnopyranoside derivatives, *Orbital: The Electronic Journal of Chemistry*, Vol.6, No.1, 20-28.
- [11] Perinelli, D. R., Lucarini, S., Fagioli, L., Campana, R., Vllasaliu, D., Duranti, A., & Casettari, L. (2018). Lactose oleate as new biocompatible surfactant for pharmaceutical applications, *European Journal of Pharmaceutics and Biopharmaceutics*, Vol.124, 55-62.
- [12] Lee, S. -M., Sandhu, G., & Walsh, M. K. (2017). Growth inhibitory properties of lactose fatty acid esters, *Saudi Journal of Biological Sciences*, 24, 1483-1488.
- [13] Kabir, A. K. M. S., Matin, M. M., Hossain, M. L., & Anwar, M. N. (2003). Antimicrobial activities of some mannofuranoside derivatives, *The Chittagong University Journal of Science*, Vol.27, No.1&2, 119-124.

- [14] Kabir, A. K. M. S., Matin, M. M., & Rahman, M. M. (1996). Selective benzylation of methyl α -D-mannopyranoside using the dibutyltin oxide and direct methods, *Chittagong University Studies, Part II: Science*, Vol.20, No.2, 99-104.
- [15] Kabir, A. K. M. S., Matin, M. M., Bhuiyan, M. M. R., & Rahim, M. A. (2001). Synthesis and characterization of some acylated derivatives of D-mannose, *The Chittagong University Journal of Science*, Vol.25, No.1, 65-73.
- [16] Kabir, A. K. M. S., Matin, M. M., (1998). Synthesis and characterization of some D-mannose derivatives, *The Chittagong University Journal of Science*, Vol.22, No.1, 105-110.
- [17] Kabir, A. K. M. S., Matin, M. M., Hossain, A., & Sattar, M. A. (2003). Synthesis and antimicrobial activities of some rhamno-pyranoside derivatives, *Journal of the Bangladesh Chemical Society*, Vol.16, No.2, 85-93.
- [18] Matin, M. M. (2006). Synthesis of some silyl protected 1,4-galactonolactone derivatives, *Journal of Applied Sciences Research*, Vol.2, No.10, 753-756.
- [19] Lawandi, J., Rocheleau, S., & Moitessier, N. (2016). Regioselective acylation, alkylation, silylation and glycosylation of monosaccharides, *Tetrahedron*, Vol.72, 6283-6319.
- [20] Kabir, A. K. M. S., & Matin, M. M. (1994). Regioselective acylation of a derivative of L-rhamnose using the dibutyltin oxide method, *Journal of the Bangladesh Chemical Society*, Vol.7, No.1, 73-79.
- [21] Matin, M. M., Hasan, M. S., Uzzaman, M., Bhuiyan, M. M. H., Kibria, S. M., Hossain, M. E., & Roshid, M. H. O. (2020). Synthesis, spectroscopic characterization, molecular docking, and ADMET studies of mannopyranoside esters as antimicrobial agents, *Journal of Molecular Structure*, Vol.1222, 128821.
- [22] Zhang, X., Wei, W., Cao, X., & Feng, F. (2014). Characterization of enzymatically prepared sugar medium-chain fatty acid monoesters, *Journal of the Science of Food and Agriculture*, Vol.95, No.8, 1631-1637.
- [23] Awual, M. R., & Hasan, M. M. (2015). Colorimetric detection and removal of copper(II) ions from wastewater samples using tailor-made composite adsorbent, *Sensors and Actuators B: Chemical*, Vol.206, 692-700.
- [24] Awual, M. R. (2017). Novel nanocomposite materials for efficient and selective mercury ions capturing from wastewater, *Chemical Engineering Journal*, Vol.307, 456-465.
- [25] Matin, M. M., Chakraborty, P., Alam, M. S., Islam, M. M., Haneef, U. (2020). Novel mannopyranoside esters as sterol 14 α -demethylase inhibitors: Synthesis, PASS prediction, molecular docking, and pharmacokinetic studies, *Carbohydrate Research*, Vol.496, 108130.
- [26] Matin, M. M., Nath, A. R., Saad, O., Bhuiyan, M. M. H., Kadir, F. A., Hamid, S. B. A., Alhadi, A. A., Ali, M. E., & Yehye, W. A. (2016). Synthesis, PASS-prediction and *in vitro* antimicrobial activity of benzyl 4-O-benzoyl- α -L-rhamnopyranoside derivatives. *International Journal of Molecular Sciences*, Vol.17, No.9, 1412.
- [27] Chowdhury, S. A., Chakraborty, P., Kawsar, S. M. A., Bhuiyan, M. M. H., & Matin, M. M. (2018). Regioselective acylation, PASS prediction and antimicrobial properties of some protected glucopyranosides. *Journal of Bangladesh Chemical Society*, Vol.30, No.1, 1-9.
- [28] Bauer, A. W., Kirby, W. M. M., Sherris, J. C., & Turck, M. (1966). Antibiotic susceptibility testing by a standardized single disk method, *American Journal of Clinical Pathology*, Vol.45, 493-496.
- [29] Matin, M. M., Bhattacharjee, S. C., Hoque, M. S. & Ahamed, F. (2019). Antibacterial activity of some medicinal plants against carbapenem-resistant *Acinetobacter baumannii* isolated from patients. *European Journal of Pharmaceutical and Medical Research*, Vol.6, No.7, 111-116.
- [30] Matin, M. M., Bhuiyana, M. H., Hossain, M., & Roshid, M. H. O. (2015). Comparative antibacterial activities of some monosaccharide and disaccharide benzoates, *Orbital: The Electronic Journal of Chemistry*, Vol.7, No.2, 160-167.
- [31] Grover, R. K., & Moore, J. D. (1962). Toximetric studies of fungicides against the brown root organisms, *Sclerotinia fructicola* and *S. laxa*, *Phytopathology*, Vol.52, 876-80.
-

- [32] Matin, M. M., Ibrahim, M., & Rahman, M. S. (2008). Antimicrobial evaluation of methyl 4-*O*-acetyl- α -L-rhamnopyranoside derivatives, *The Chittagong University Journal of Biological Sciences*, Vol.3, No.1&2, 33-43.
- [33] Rahim, A., Bhuiyan, M. M. H., & Matin, M. M. (2020). Microwave assisted efficient synthesis of some flavones for antimicrobial and ADMET studies. *Journal of Scientific Research*, Vol.12, No.4, 673-685,
- [34] Frisch, M. J., Trucks, G. W., Schlegel, H. B., Scuseria, G. E., Robb, M. A., Cheeseman, J. R., Scalmani, G., Barone, V., Petersson, G. A., & Nakatsuji, H. (2013). Gaussian 09, Gaussian Inc. (Wallingford CT).
- [35] Pires, D. E. V., Blundell, T. L., & Ascher, D. B. (2015). pkCSM: predicting small-molecule pharmacokinetic properties using graph-based signatures, *Journal of Medicinal Chemistry*, Vol.58, No.9, 4066–4072.
- [36] Daina, A., Michielin, O., & Zoete, V. (2017). SwissADME: a free web tool to evaluate pharmacokinetics, drug-likeness and medicinal chemistry friendliness of small molecules, *Scientific Report*, 7, 42717.
- [37] Matin, M. M. (2008). One step intramolecular cyclization of diol via mesylation: efficient synthesis of sugar derived [1,4]oxazepanes, *Journal of Bangladesh Chemical Society*, Vol.21, No.2, 179-183.
- [38] Matin, M. M. (2006). *N*-Butylation and -acetylation of a sugar derived β -aminoester. *The Chittagong University Journal of Science*, Vol.30, No.1, 35-39.
- [39] Ditchfield, R., Hehre, W. J., & Pople, J. A. (1971). Self-consistent molecular orbital methods-9: Extended Gaussian-type basis for molecular-orbital studies of organic molecules, *Journal of Chemical Physics*, Vol.54, 724.
- [40] Lipinski, C. A., Lombardo, F., Dominy, B. W., & Feeney, P. J. (1997). Experimental and computational approaches to estimate solubility and permeability in drug discovery and development settings, *Advanced Drug Delivery Reviews*, Vol.23, 3-25.